NONLINEAR SPECTRAL MIXTURE MODELING OF LUNAR MULTISPECTRAL: IMPLICATIONS FOR LATERAL TRANSPORT

John F. Mustard, Lin Li, and Guoqi He,
Department of Geological Sciences,
Box 1846,
Brown University,
Providence RI, 02912.

Corresponding Author: John F. Mustard
Phone: 401-863-1264
Fax: 401-863-3978
Email: John_Mustard@brown.edu

Abstract

Linear and nonlinear spectral mixture models applied to Clementine multispectral images of the Moon result in roughly similar spatial distributions of endmember abundances. However, there are important differences in the absolute values of the predicted abundances. The magnitude of these differences and the implications for understanding geological processes are investigated across a geologic contact between mare and highland in the Grimaldi Basin on the western nearside of the Moon. Vertical and lateral mass transport due to impact cratering has redistributed mare and highland materials across the contract, creating a gradient in composition. Solutions to linear and nonlinear spectral mixture models for identical spectral endmembers of mare, highland, and fresh crater materials are compared across this simple geologic contact in the Grimaldi Basin. Profiles of mare abundance across the contact are extracted and compared quantitatively. Profiles from the linear mixture models indicate that the geologic contact has an average mare abundance of 60%, and the compositional boundary is asymmetric with more mare transported onto the highland side of the contact than highland onto the mare side of the contact. In contrast the nonlinear abundance profiles indicate that the geologic contact has an average mare abundance of 50%, and the compositional boundary is remarkably symmetric. Given the expectation that materials will be intimately mixed on the surface of the Moon, and that the asymmetries implied by the linear model are not consistent with our understanding of lunar surface processes, the nonlinear spectral mixture model is preferred and should be applied whenever quantitative abundance information is required. The remarkable symmetry in the compositional gradients across this contact indicate that lateral mass transport dominates over vertical transport at this boundary is that vertical transport.

Introduction

Spectral mixture analysis (SMA) of lunar spectroscopic and multispectral data has been used with great success in a wide variety of applications on the Moon [Pieters et al, 1985; Bell and Hawke, 1995; Tompkins et al., 1994; Head et al., 1993; Mustard and Head, 1996; Blewitt et al., 1995; Li et al., 1996; Staid et al., 1996]. All published applications of SMA to lunar multispectral imaging data, without exception, use linear mixture modeling. For linear mixture modeling to be strictly valid, the endmember materials that are mixed must be arranged in physically discrete patches, as in a checkerboard. This assumption is probably not valid for typical endmember materials on the surface of the Moon. As has been demonstrated through numerous analysis of soils and cores from the Apollo landing sites (e.g. Heiken et al., 1991), the lunar surface is an intimate mixture of several lithologies, some of which have been transported over large distances. The process responsible for this mixing is meteorite bombardment of the surface which, through the impact process, causes lunar materials to be disaggregated and redistributed on the surface. The spectral mixture systematics within an intimate mixture of endmember materials is well known to be a nonlinear problem [Hapke, 1993; Johnson et al., 1983; Mustard and Pieters, 1987; 1989].

If the objectives of an analysis of lunar spectral data are primarily to identify the spatial distributions of components and some general understanding of the physical abundance, then the linear mixture model approach is adequate. If, however, the objectives are to quantitatively determine the spatial relationships and physical abundances of components, and to understand and model processes responsible for the observations, then it is important to critically assess the linear assumption and employ a nonlinear mixture model if warranted. The difference in abundances between a linear and nonlinear solution can be significant, and may change the interpretation of the processes at work [Herzog and Mustard, 1996].

In this analysis, linear and nonlinear mixture models are applied to Clementine UV-VIS multispectral data of a mare-highland boundary. In a related investigation, we are studying the magnitude of material transport across these boundaries [e.g. Li et al., 1997]. Mare-highland boundaries provide an excellent environment to examine mixing relationships since mare and

3

highland have distinct compostions and spectral properties, the geologic contact is sharp, and formed in a relatively short period of time.

The investigation of the composition of mare-highland boundaries carried out by Mustard and Head [1996] using multispectral images from the Galileo Solid State Imaging (SSI) instrument revealed the existence of three distinct mixing systematics across the mare-highland contacts in the region of southwestern Procellarum. The three basic types are narrow, moderate, and complex mixing gradients, and each implies a different set of fundamental processes that have contributed to the observed gradients. Although the 4 km resolution of the Galileo SSI data was too low to critically evaluate the exact properties of these boundaries, particularly in areas with rapidly changing abundances, it was recognized that mare-highland contacts in the Grimaldi Basin exhibited a very sharp compositional boundary. This was interpreted to indicate that the boundary has been affected only by modest post-formation redistribution of material by impact processes.

The high spatial resolution and multispectral data acquired of Clementine UV/VIS camera (120 m/pixel, 5 filters between 0.415- 1.0 μm) allows the relatively simple contact of mare and highland in the Grimaldi Basin to be analyzed in more detail. Both linear and nonlinear spectral mixture models are applied to these data and the results compared. The results show that the interpretation of lunar surface processes are fundamentally different between the linear and nonlinear solutions, and that the nonlinear spectral mixture model is more appropriate than a linear model for lunar applications.

Calibration of Clementine Data:

Orbit 61 crossed directly over the Grimaldi Basin by the western nearside of the Moon (Figure 1). Five filters from the Clementine UV-VIS camera covering a 10° latitude swath across the basin were co-registered, mosaicked, and calibrated using the standard methods developed by the Clementine team [Pieters et al., 1994; Pieters, 1995]. Briefly, this involves corrections for gain and offset, dark current, frame transfer, flat field, photometric correction, and spectral calibration. The reflectance calibration involves the use of laboratory reflectance measurements of an Apollo 16 soil sample. These measurements are made relative to a halon reference target measured under

4

identical illumination, and then corrected for the absolute reflectance of halon. Following this calibration, the data are within 5% of absolute, and have been normalized to observation geometry with the incidence angle, i=30° and emergence angle, e=0°. This photometric normalization is based on a highly generalized model for the photometric behavior of the lunar surface, and is the most valid for original observations with 20°< i < 40°. The incidence angle for these observations was generally greater than 24°.

Mixture Modeling:

The basic approach of mixture modeling is to fit, using the technique of least squares, a suite of spectral endmembers to an observed spectrum, subject to the constraint that the sum of the fractions is equal to 1.0 [Adams et al., 1993]. As long as the number of endmembers does not exceed the number of spectral channels, a solution exists, though for the lunar surface the number of endmembers is generally less than the five UV-VIS channels. In typical applications three endmembers are resolved: one each for mare, highland, and fresh crater materials. In complex or spectrally diverse areas, an additional mare, highland, or fresh crater endmember may be resolved, but not all three.

Linear SMA is only strictly valid if the path length of photons in the particulate surface is less than the scale of mixing. Intimate mixing refers to the case where the photon path length exceeds the scale of mixing. This is the expected case for much of the lunar surface [Heinken, et al, 1991]. Although the reflectance of an intimate mixture is a nonlinear combination of the reflectances of the endmembers in the mixture, the mixing systematics are predicted to be linear if the reflectances are converted to single-scattering albedo [Hapke, 1993; Hapke, 1981]. Thus the same general approach as SMA is employed in nonlinear spectral mixture modeling, except the calibrated reflectance data are converted to single-scattering albedo (SSA) before selecting endmembers and computing fractions. To convert to SSA, we employ the equations of [Hapke, 1993] for radiance coefficient, subject to the following assumptions: the opposition surge is negligible at the i=30° and e=0° geometry, and the lunar surface scatters light isotropically. The second assumption is

justified on the basis that many surfaces approximate lambertian behavior at i=30° and e=0°
[Mustard and Pieters, 1989].

Both linear and nonlinear image-based spectral mixture models were applied to southern mare-highland boundary in Grimaldi (Figure 1). The northern boundary is modified by the large crater Grimaldi B that impacted directly on the mare-highland boundary. In the image-based approach the spectral endmembers are selected directly from the image data, and are thus internally consistent. Three endmembers are required: mare, highland, and fresh crater. The mare and highland endmembers were selected from homogeneous regions far from the contact. The fresh crater endmember accounts for the changes in the spectral properties of lunar materials due to space weathering. Identical locations were used for the endmembers in the linear and nonlinear SMA. In general, the average RMS error of the solutions is lower for the nonlinear than the linear approaches (1% for linear, 0.2% for nonlinear), but the spatial information in the RMS error images is unchanged.

Results for the Grimaldi Basin Mare-Highland Boundary:

Profiles of mare abundance, orthogonal to the geologic contact between mare and highland, were extracted from the mare fraction data determined with the linear and nonlinear mixture models. The abundance of highland is essentially the mirror image of the mare abundance. Four representative profiles, the locations of which are shown in Figure 1, are presented in Figure 2. These abundance profiles are 16-pixel wide averages along the length of the profile. The averages are used to suppress random noise and high frequency variations in the mare abundance caused by local geological processes.

The geologic contact is an important reference point for this analysis. The relative surface abundance of mare on either side of the contact is a function of vertical and lateral mass transport due to impact processes. Thus the symmetry of the abundance profiles relative to the geologic contact will be important. If vertical transport is important, then the abundance profiles should exhibit a strong asymmetry with a greater amount of highland on the mare side of the contact than mare on the highland side of the contact. Conversely, a symmetric profile is expected if lateral

transport dominates over vertical transport. The location of the geologic contact was defined through photogeologic mapping on Lunar Orbiter IV images which have better spatial resolution than the Clementine data. This Clementine data were co-registered to Lunar Orbiter images and the position of the geologic contact was transferred to the Clementine data. The profiles shown in Figure 2 have been positioned such that the pixel locations of the geologic contacts are identical.

The linear and nonlinear profiles of mare abundance across the geologic contact exhibit similar overall characteristics. At distances greater than 10 km from the contact, there is a general increase (mare side) or decrease (highland side) that is approximately linear with distance. Within 10 km of the contact, the mare abundances exhibit more rapid changes as a function of distance, with the most rapid rate of change within 2 km of the contact. Detailed modeling of these abundance profiles is currently under investigation [e.g. Li et al., 1997].

Though similar in overall character, the linear and nonlinear abundances exhibit important differences. At the geologic contact, the nonlinear mixture model determines that the abundance of mare 50%, while for the linear mixture model the abundance is typically 60% [Li et al., 1997]. This has been determined for a number of different regions along the contact, and the average values are presented in Table 1. The maximum difference between the linear and nonlinear solutions is where the nonlinear mare abundance is 50%. This is illustrated in Figure 3 where the difference between nonlinear and linear mare abundances is plotted as a function of distance. Note, however, that although the maximum difference is approximately at the geologic contact, overall the abundances show the greatest difference on the highland side of the contact.

The relationships between the linear and nonlinear solutions are expected from theoretical considerations. In general, low albedo (e.g. mare) materials dominate the reflectances of intimate mixtures, thereby causing a linear mixture model to over predict the abundance of the low albedo constituent. As shown in Figure 3, this leads to the maximum differences on the highland side of the geologic contact. The differences impact in a fundamental way the interpretations of the processes responsible for the observed abundance distributions, discussed in detail below.

7

The different mixing model solutions also affect the apparent symmetry of the compositional gradients across this contact. This is demonstrated in Figure 4. Each of the profiles 1 through 4 is plotted as a solid line, where the linear solutions are in Figure 4a and the nonlinear solutions in Figure 4b. To demonstrate symmetry, each profile is inverted about the geologic contact and plotted on a reverse scale as dotted lines. A compositional boundary that is symmetric about the geologic contact should result in overlapping profiles, and one that has asymmetries will exhibit discrepancies. It is clear from Figure 4 that the mare abundance profiles from the nonlinear mixture model are much more symmetric than those from the linear mixture model. This appears to be valid even as the general shape of the profiles changes along the strike of the geologic contact. For example, Profile 3 has a narrower steep mixing zone and a more extended moderate mixing zone compared to the other profiles, and yet the symmetry of the profile is preserved.

Each of the profiles shown in the previous figures, although averages of 16 pixels wide, nevertheless exhibits variability due to the noise of the Clementine UV-VIS camera and small scale geologic variations. To minimize this variability in the profiles and to allow the more global properties of the compositional variation across the boundary to be observed, an average mare abundance profile is extracted that encompasses the entire western portion of the Clementine mosaic. Here the geologic contact is approximately linear and orthogonal to the profile direction. The profiles for the linear and nonlinear solutions are shown in Figure 5, plotted in a similar manner to Figure 4. Since it was evident from the other profiles that the geologic contact occurs at approximately 50% in the nonlinear profiles, the pixel that corresponds to the 50% point was used as a proxy for the geologic contact and hence the axis of symmetry.

It is clear that, compared to the linear mixing model, the nonlinear approach results in a highly symmetric mixing profile (Figures 4 and 5). However, it is important to consider whether the nonlinear results are more valid than the linear results. On the basis of a priori physical arguments (e.g. soil composition, texture, and mixing observed in lunar samples, [Heiken et al., 1991]), the nonlinear approach is more appropriate given the intimate mixing of soil constituents. The abundance profiles from the linear solutions are asymmetric and indicate that the amount of mare

transported to the highlands is greater than the amount of highland transported to the mare. This is contrary to the expected distributions at a simple geologic contact like in the Grimaldi Basin based on three geologic relationships. 1) The highlands are topographically higher than the mare, and thus gravity and slope effects should results in a greater down slope movement of highland material than an up slope movement of mare material. 2) If vertical mixing is important, this favors more highland material on the mare side due to excavation of highland substrate beneath the thin mare cover near the geologic contact. 3) Cratering efficiencies in the highlands should be greater than in the mare, thus favoring a greater transport of highland material for equivalent impactor size.

Conclusions:

Clearly, the interpretation of the physical processes causing mixing across mare-highland boundaries is strongly affected by the choice of linear vs nonlinear mixture analysis. For the linear solutions, the mixing systematics are asymmetric, with much more mare apparently transported to the highlands, and the mare abundance at the geologic contact is 60%. This result is contrary to expectation, as most models for lateral transport would predict the opposite. For the nonlinear solutions, however, the mixing process is apparently very symmetric. The geologic contact occurs where the mare abundance is 50%, and equal amounts of mare are transported to the highlands as are highlands to the mare.

On the basis of these observations and arguments, we conclude that it is critical to employ a nonlinear spectral mixture model when the specific abundances of materials is important. The nonlinear model results for the mare-highland contact in the Grimaldi Basin demonstrate a remarkable symmetry to the compositional gradients across this boundary. This symmetry indicates that vertical mixing is unimportant for this boundary, and that mare transport to the highlands is approximately similar to highland transport to the mare. The mare abundance profiles across the boundary exhibit a coherent set of characteristics, regardless of the specific location and local geologic relationships along the contact (steep gradients within a few kilometers of the

contact, extended gentle gradients up to 40 km from the contact). These basic characteristics are analogous to diffusion profiles, and we are currently investigating the applicability of diffusion approximations to lateral mass transport across compositional boundaries on the Moon (Li et al., 1997).

Table 1. Average Mare Abundance at the Geologic Contact for 10 Profiles

Mixture Model	Mare Abundance	Standard Deviation
Linear	62.162%	4.08
Nonlinear	51.79	3.59

References:

Adams, J. B., M. O. Smith, and A. R. Gillespie, in *Remote Geochemical Analysis: Elemental and Mineralogical Composition*, Cambridge Press, pp. 145-166, 1993.

Bell, J. F. and B. R. Hawke, Compositional variability of the Serenitatis/Tranquillitatis region of the Moon from telescopic multispectral imaging and spectroscopy, Icarus 118, 51-68, 1995.

Blewitt, D. T., B. R. Hawke, P. G. Lucey, G. J. Taylor, R. Jaumann, and P. D. Spudis, Remote sensing and geologic studies of the Schiller-Schickard region of the Moon, J. Geophys. Res., 100, 16959-16972, 1995.

Hapke, B., Bidirectional reflectance spectroscopy 1: Theory, J. Geophys. Res. 86, 3039-3054, 198 1 .

Hapke, B. *Theory of Reflectance and Emittance Spectroscopy*, Cambridge Press, 1993.

Head, J. W., S. Murchie, J. F. Mustard, C. M. Pieters, G. Neukum, A. McEwen, R. Greeley, and M. J. S. Belton, Lunar impact basins: New data for the western limb and farside (Orientale and South Pole-Aitken Basins) from the first Galileo flyby, J. Geophys. Res. 98, 17149-17182, 1993.

Heiken, G., D. Vaniman, and B. French, *Lunar Sourcebook; A Users's Guide to the Moon*, Cambridge Press, 736 pp., 1991.

Herzog, S. G., and J. F. Mustard, Reflectance spectra of five-component mineral mixtures: Implications for mixture modeling, Lunar and Planetary Science XXVII, 535-536, 1996.

Johnson, P.E., M.O. Smith, S. Taylor-George, and J.B. Adams, A semiempirical method for analysis of the reflectance spectra of binary mineral mixtures, J. Geophys. Res, 88, 3357-3361, 1983.

Li, L., J. F. Mustard, and G. He, Compositional gradients across Mare-Highland contacts: The importance of lateral mixing, Lunar and Planetary Science XXVIII, 811-812, 1997.

L. Li, Mustard, J. F., and G. He, Mixing across simple mare-highland contacts: New insights from Clementine UV-VIS data of the Grimaldi basin, Lunar and Planetary Science XXVII, 751-752, 1996.

Mustard, J.F. and J. W. Head Mare-highland mixing relationships along the southwestern shores of Oceanus Procellarum, J. Geophys. Res. 101, 18,913-18,925, 1996.

Mustard, J. F., and C. M. Pieters, Photometeric phase functions of common geologic minerals and applications to quantitative analysis of mineral mixture reflectance spectra, J. Geophys. Res. 94, 13,619- 13634, 1989.

Mustard, J. F., and C. M. Pieters, Quantitative abundance estimates from bidirectional reflectance measurements, Proc. 17th Lunar Planet. Sci. Conf., J. Geophys. Res., 92, E617-E626, 1987.

Tompkins, S., C. M. Pieters, J. F. Mustard, P. Pinet, and S. D. Chevrel, Distribution of materials excavated by the lunar crater Bullialdus and implication of the geologic history of the Nubium region, Icarus 110, 261-274, 1994.

Pieters, C. M., J. B. Adams, P. Mouginis-Mark, S. H. Zisk, M. O. Smith, J. W. Head, T. B. McCord, The nature of crater rays: The Copernicus example, J. Geophys. Res. 90, 12,393-12413, 1985.

Pieters, C.M., M.I. Staid, E.M. Fischer, S. Tompkins and G. He, A sharper view of impact craters from Clementine data, Science, 266, 1,844-1,848, 1994.

Pieters, C. M., G. He, M. Staid, S. Tompkins, and E. M. Fischer, Clementine UV-VIS Data Calibration and Processing, URL: http://www.planetary.brown.edu/clementine/ calibration.html, 1995.

Staid, M.I., C.M. Pieters and J.W. Head, Mare Tranquillitatis: Basalt emplacement history and relation to lunar samples, J. Geophys. Res, 101, 23,213-23,228, 1996.

Figure Captions:

Figure 1:   a) Generalized geologic map of the Grimaldi region showing the outlines of major

impact and tectonic features. The dashed line indicates the region for which

Clementine UV-VIS data have been processed and analyzed.b) Clementine 750 nm

mosaic of the study area. The locations of the four primary profiles are indicated.

Figure 2:   Profiles of mare abundance across the geologic contact between mare and highland

along the southern boundary of the Grimaldi Basin. The locations for the profiles

are shown in Figure 1a. Solid lines show the mare abundances determined using

the nonlinear spectral mixture model; dashed lines show the abundances determined

using the linear spectral mixture model. The profiles have been offset 50% for

clarity, and the horizontal orientations have been shifted such that the location of the

geologic contact lines up. Distance is measured from the geologic contact.

Figure 3:   Difference between the mare abundance calculated with the nonlinear spectral

mixture model and the abundance determined with the linear spectral mixture

model, for the abundance profiles shown in Figure 2. The difference profiles have

been offset by 10% for clarity. Distance is measured from the geologic contact.

Figure 4:   Mare abundance profiles determined from the linear and nonlinear spectral mixture

models (solid lines) plotted together with the same profiles but with the horizontal

and vertical axes reversed (dashed lines). Perfectly symmetric mixing processes

would result in overlapping profiles (e.g. nonlinear mixing) while asymmetric

processes would not result in overlapping profiles (e.g. linear mixing).

Figure 5:   Mare abundance profiles for the western half of the study area where the geologic

contact is approximately linear and runs east-west. As in Figure 4, the solid line the

actual abundance profile while the dashed line shows the same profile but with the

distance and abundance axes reversed. The nonlinear spectral mixture model

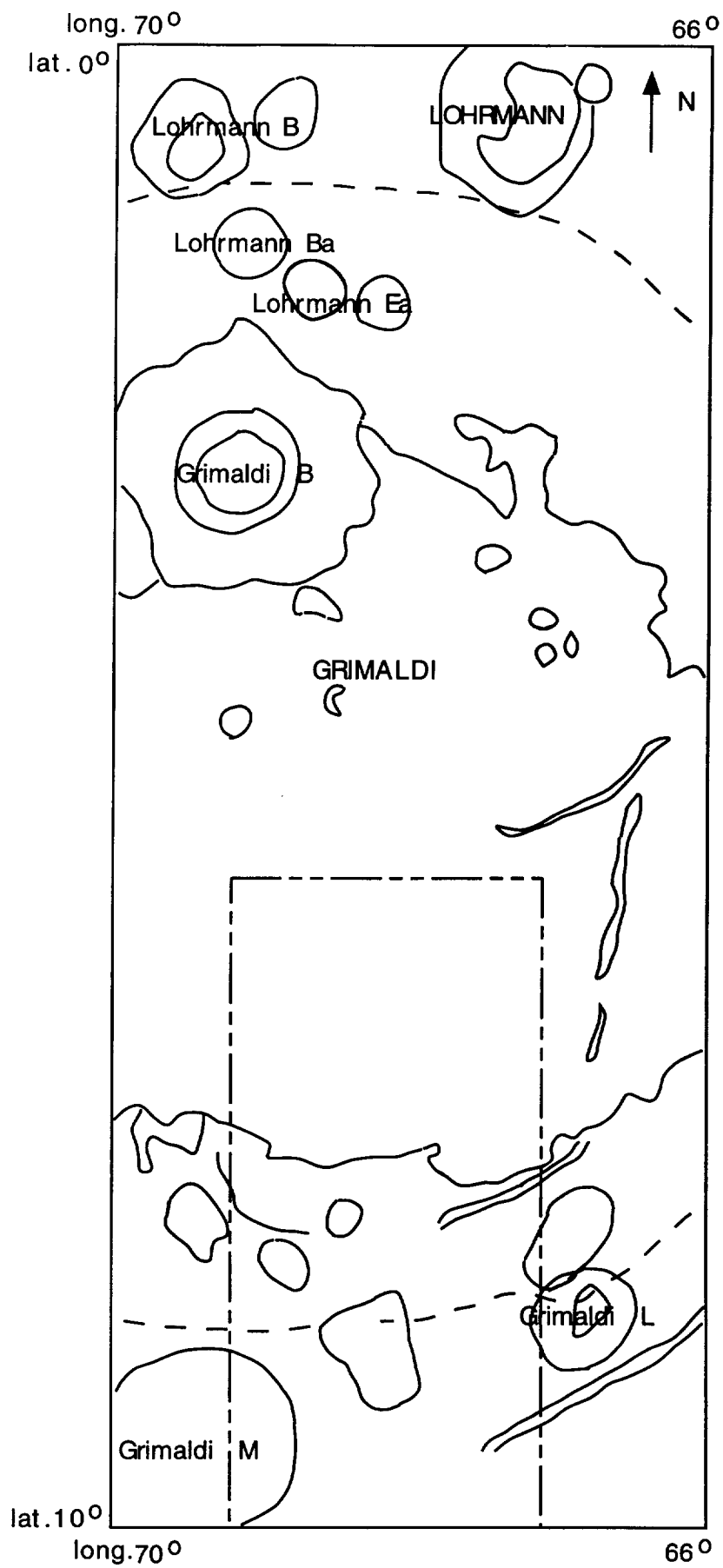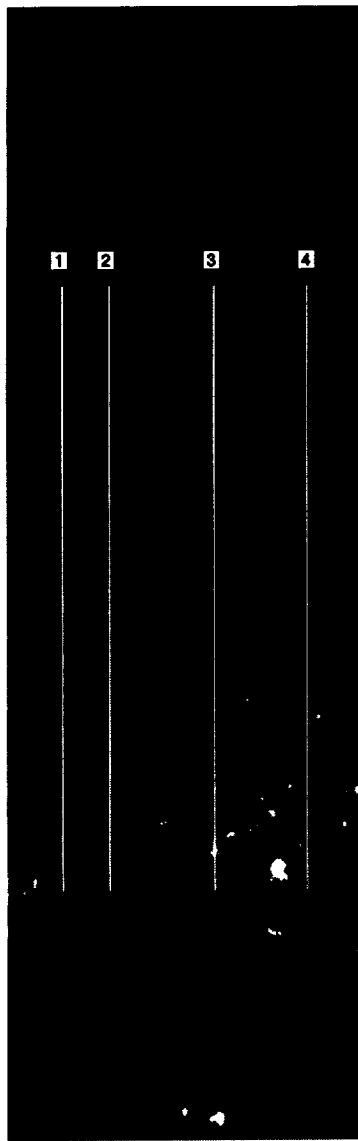results in a highly symmetric compositional boundary.

13

long. 70°   66°
lat. 0°

Lohrmann B   LOHRMANN   ↑ N

Lohrmann Ba

Lohrmann Ea

Grimaldi B

GRIMALDI

Grimaldi L

Grimaldi M

lat. 10°
long. 70°   66°

Fig.1 Geologic sketch map of Grimaldi region
(1 :2000000)

(1a)

Clementine 750 µm mosaic of Mare-Highland boundary
along the southern edge of Grimaldi Basin. Locations
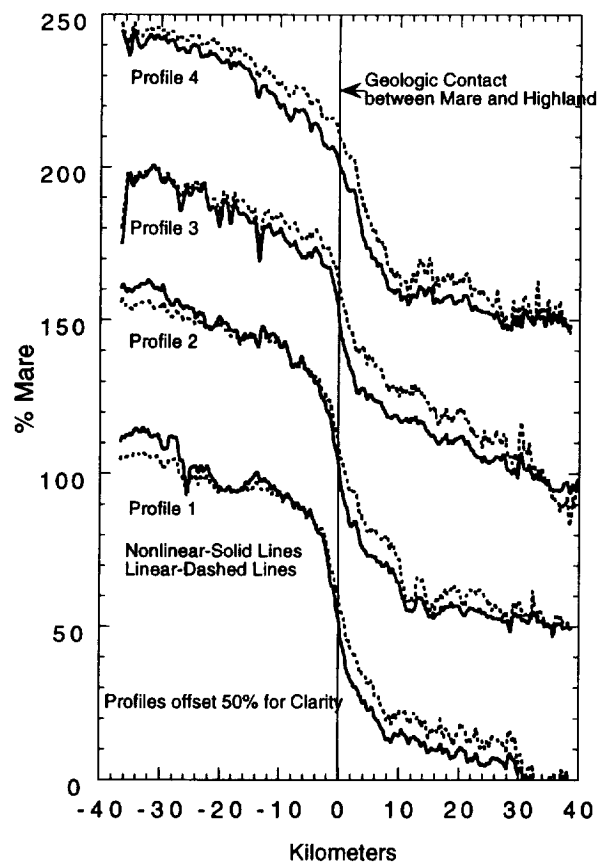of the 4 profiles used in this poster indicated by the lines.
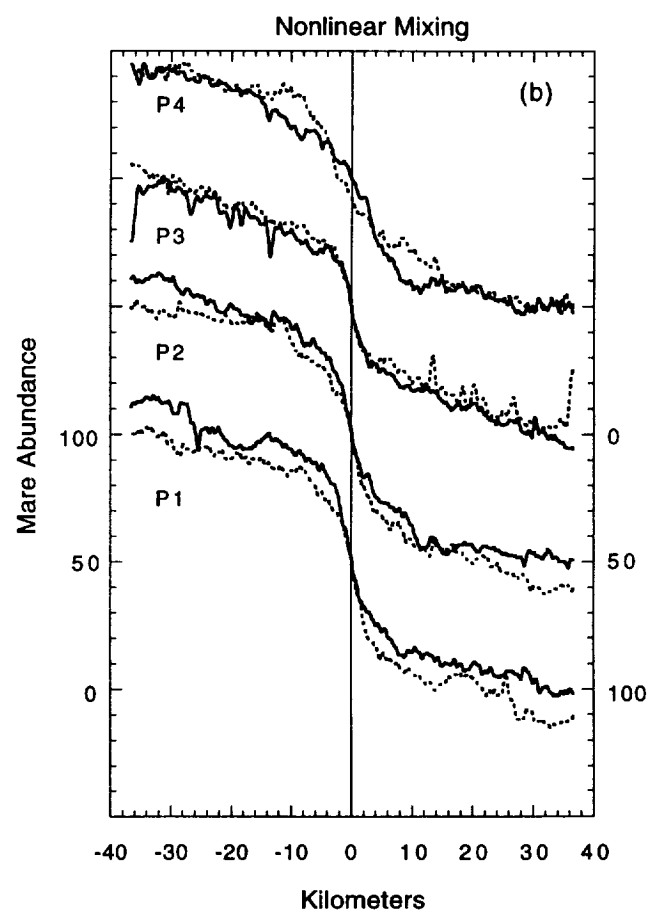Pixel Size: ≈120 meters Image width: 45 km

(16)

Figure 2

Figure 3
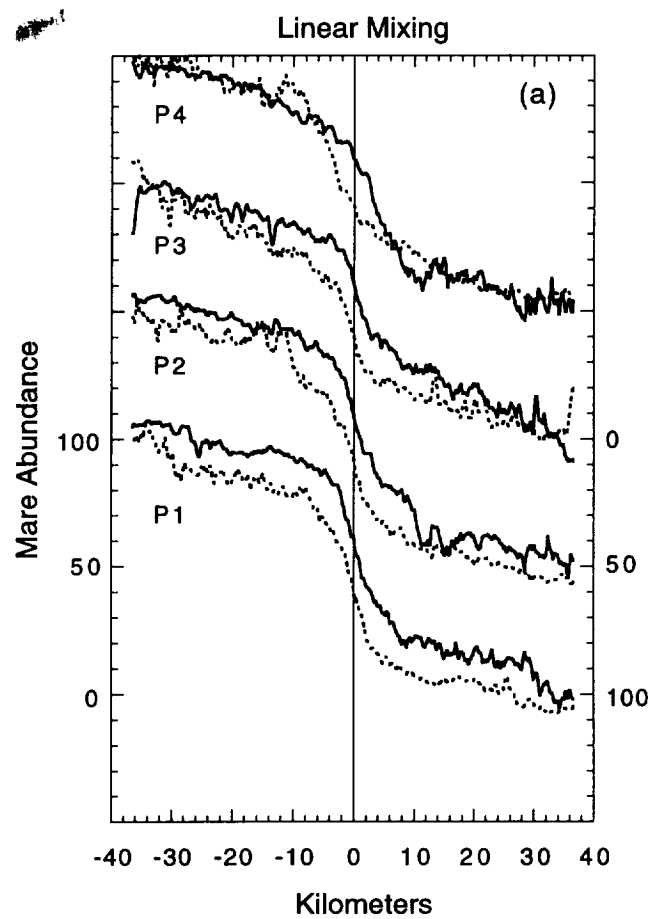
Linear Mixing

(a)

P4

P3

P2

Mare Abundance

100

50

0

P1

-40 -30 -20 -10 0 10 20 30 40

Kilometers

0

50

100

Nonlinear Mixing

(b)

P4

P3

P2

Mare Abundance

100

50

0

P1

-40 -30 -20 -10 0 10 20 30 40

Kilometers

0

50

100

Figure 4

Figure 5